


RESEARCH ARTICLES

Open Access



Development of personalized non-invasive ventilation masks for critically ill children: a bench study

Rosemijne R. W. P. Pigmans^{1,2*} , Rozalinde Klein-Blommert¹, Monica C. van Gestel¹, Dick G. Markhorst¹, Peter Hammond^{3,4}, Pim Boomsma⁵, Tim Daams⁵, Julia M. A. de Jong⁵, Paul M. Heeman⁵, Job B. M. van Woensel^{1,2}, Coen D. Dijkman⁵ and Reinout A. Bem^{1,2}

Abstract

Background Obtaining a properly fitting non-invasive ventilation (NIV) mask to treat acute respiratory failure is a major challenge, especially in young children and patients with craniofacial abnormalities. Personalization of NIV masks holds promise to improve pediatric NIV efficiency. As current customization methods are relatively time consuming, this study aimed to test the air leak and surface pressure performance of personalized oronasal face masks using 3D printed soft materials. Personalized masks of three different biocompatible materials (silicone and photopolymer resin) were developed and tested on three head models of young children with abnormal facial features during preclinical bench simulation of pediatric NIV. Air leak percentages and facial surface pressures were measured and compared for each mask.

Results Personalized NIV masks could be successfully produced in under 12 h in a semi-automated 3D production process. During NIV simulation, overall air leak performance and applied surface pressures were acceptable, with leak percentages under 30% and average surface pressure values mostly remaining under normal capillary pressure. There was a small advantage of the masks produced with soft photopolymer resin material.

Conclusion This first, proof-of-concept bench study simulating NIV in children with abnormal facial features, showed that it is possible to obtain biocompatible, personalized oronasal masks with acceptable air leak and facial surface pressure performance using a relatively short, and semi-automated production process. Further research into the clinical value and possibilities for application of personalized NIV masks in critically ill children is needed.

Keywords Face mask, Customization, 3D printing, Acute respiratory failure, Non-invasive respiratory support, Pediatric intensive care unit

*Correspondence:

Rosemijne R. W. P. Pigmans
r.r.pigmans@amsterdamumc.nl

Full list of author information is available at the end of the article



© The Author(s) 2024. **Open Access** This article is licensed under a Creative Commons Attribution 4.0 International License, which permits use, sharing, adaptation, distribution and reproduction in any medium or format, as long as you give appropriate credit to the original author(s) and the source, provide a link to the Creative Commons licence, and indicate if changes were made. The images or other third party material in this article are included in the article's Creative Commons licence, unless indicated otherwise in a credit line to the material. If material is not included in the article's Creative Commons licence and your intended use is not permitted by statutory regulation or exceeds the permitted use, you will need to obtain permission directly from the copyright holder. To view a copy of this licence, visit <http://creativecommons.org/licenses/by/4.0/>.

Background

Non-invasive ventilation (NIV) can be a valuable treatment in critically ill children with acute respiratory failure admitted to the pediatric intensive care unit (PICU) [1, 2]. A recent worldwide study reported that almost 1 out of every 4 children with pediatric acute respiratory distress syndrome currently receives this treatment [3]. One of the most important challenges in treating children with NIV is to obtain a properly fitting mask [2, 4–9]. A suboptimal seal of the NIV mask results in increased air leak, patient discomfort and the development of facial skin pressure injuries [9, 10]. These factors are associated with patient–ventilator asynchrony and reduced tolerance, contributing to NIV failure [8, 9, 11–13]. This is relevant as several large studies report NIV failure rates in the PICU to range from 25 to 53% [3, 14]. Young children are particularly exposed to ill-fitted NIV interfaces, as a result of the limited size ranges of commercially available masks. In addition, syndromic craniofacial malformations in children (a common problem in patients admitted to the PICU) might further complicate mask fitting [8, 11, 12]. Therefore, personalization of NIV masks addressing the specific facial features of the patient is believed to be a promising future approach to improve pediatric NIV efficiency [4–9].

There have been several previous explorations in the field of mask personalization [9, 15–18]. Biocompatible soft materials, like silicon, which has a cushioning effect to minimize pressure on the face and improve seal compared to hard materials, were investigated using molding techniques to produce a mask [9, 15, 16]. However, such strategies are labor and time consuming, which may limit their usefulness in the setting of acute respiratory failure. More novel, state-of-the-art techniques, such as 3D printing of soft materials may be promising to provide a more rapid, personalized NIV mask production method [6, 17, 18]. Yet, medical device research aimed at establishing 3D printed personalized masks is still in the early stage. For example, Willox et al. [18] tested 3D printed polyamide oronasal masks in three healthy adult volunteers, and found reduced air leak as compared to conventional NIV masks, but also expressed the need to test softer materials. Borrás-Novell et al. [17] tested a 3D printed, softer, silicone nasal mask in a single neonatal case, and found reduced air leak percentages. Nevertheless, before pilot and further clinical studies in children with acute respiratory failure can be attempted, further exploration of the production process, and performance of designs and materials in a preclinical setting is needed.

The aim of this study was to explore 3D printed personalized oronasal NIV face masks produced with different biocompatible soft materials, and test their air leak and facial surface pressure performance in

preclinical bench simulation of pediatric NIV. For this purpose, we developed head models of young children with abnormal facial features for a proof-of-concept study.

Methods

Development of pediatric head models

Three different head models were developed, based on the facial 3D scan of three children (aged 3–4 years) with a syndrome with accompanying characteristic facial features: Down syndrome (DS, Trisomy 21), cardiofaciocutaneous syndrome (CFCS) and velocardiofacial syndrome (VCFCS). These children were selected based on evident facial abnormalities as part of their syndrome, to provide for a proof-of-concept model to test our personalized mask design and materials. The 3D images were obtained with approval of the Joint Research and Ethics Committee of the Eastman Dental Institute/Eastman Dental Hospital Ethics Committee (JREC 00/EO42). The scans were digitally transformed into solid heads by merging the scans with the back of a standard head in Autodesk Meshmixer (version 3.5.474, Autodesk, San Rafael, CA, USA).

The pediatric head models were developed in Autodesk Inventor (Autodesk, USA). An example of a final head model as produced is shown in Fig. 1A. All three test head models are shown in Additional file 1: Figure S1. All head models were composed of four solid, 3D printed parts (ASA, Fortus 450mc Industrial FDM printer, Stratasys, Israel): the face, middle and back of the head, and the facial pressure components. Six capacitive force sensors (4.5N, calibrated, Singletact, PSS UK Limited, UK) were placed under the pressure components on a flat surface following the contours of NIV oronasal masks. The measured force was converted to pressure by dividing the output by the surface area of the corresponding pressure component. The regions for pressure measurements include the nose bridge, both sides of the nose, both cheeks and the chin. They, respectively, enclose the nasion, nasal ala left and right, chelion left and right and the sulcus inferior facial landmarks. The electronics of the sensors were placed in the back part of the head. The sensors were coupled and connected to a microcontroller (Arduino Uno, Arduino, USA). A 3-mm silicon (Ecoflex 00-20, Smooth-on, USA) layer was poured around the head to create a surface texture mimicking human skin as previously described [6]. Finally, silicon tubes were inserted through the nose and mouth cavities to create an airtight airway to be connected to a mechanical lung simulator. A more detailed example of the design and a final head model is shown in the Supplemental material, Additional file 1: Figure S2 and S3.

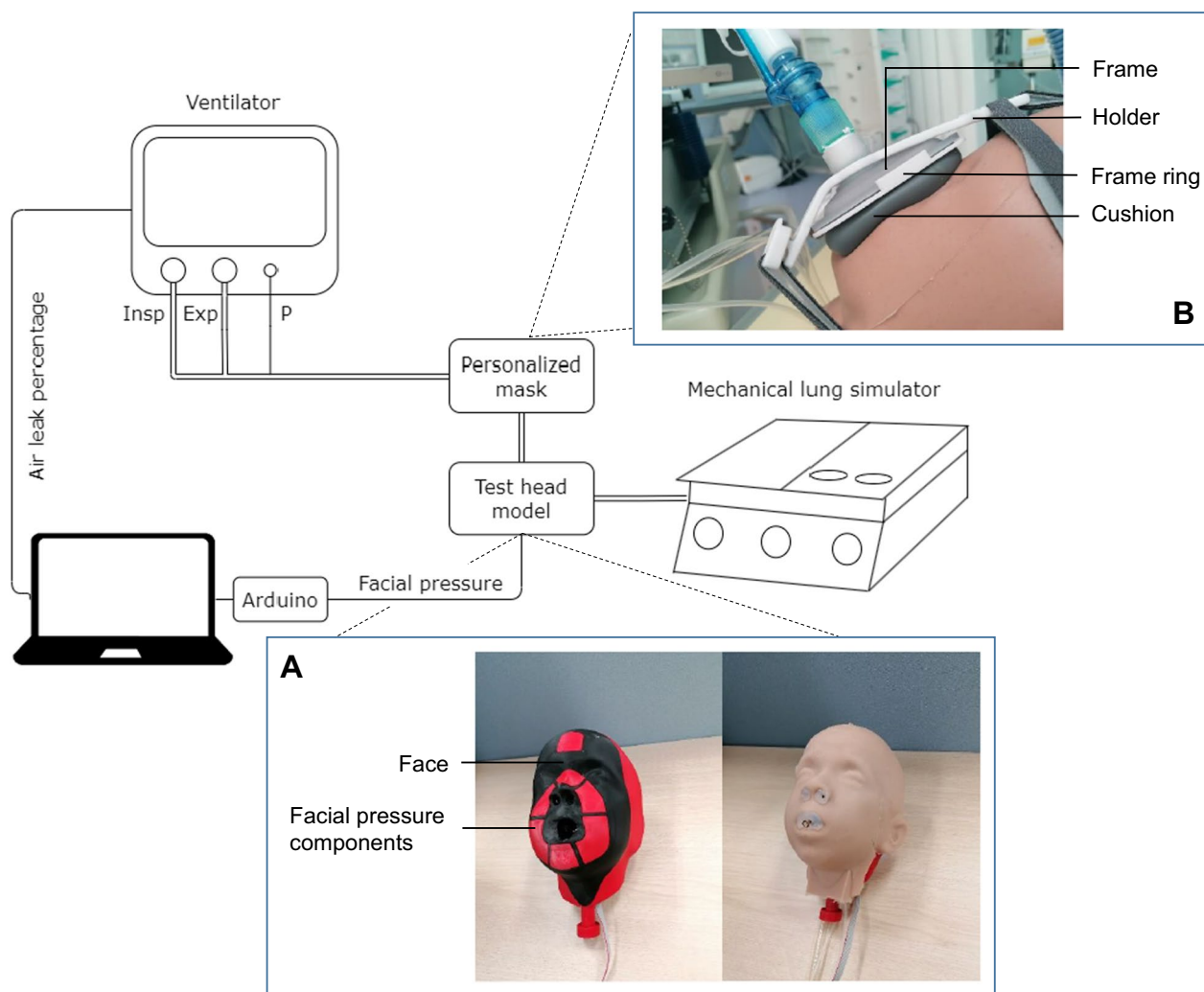


Fig. 1 A schematic overview of the bench test setup for pediatric non-invasive ventilation simulation with details on the test head model (A) and the personalized mask (B). The personalized mask consists of a frame, frame ring, holder and a personalized cushion. The mask is placed on the accompanying test head model, which contains facial pressure components that follow the outline of the ventilation mask. The pressure sensors underneath the components are connected to the laptop through a microcontroller (Arduino). The test head model has a 3-mm silicon layer to create an airtight connection to the mechanical lung simulator. The mask is connected to the ventilator, which directly provides information on the inspiration (insp) and expiration (exp) volumes, flows and pressures (P) to the laptop for data collection

Mask design

Personalized, oronasal masks were designed as a composition of three parts: a fully customized cushion, a frame and a frame ring. To assemble the mask, the cushion is placed in the frame with fixation through the frame ring (Fig. 1B and Additional file 1: Figure S4). The frame and accompanying frame ring were designed in eight different sizes for children up to 7 years old (see Additional file 1: Figure S5 and 6), as based on the DINED database [19], and on studies of Goto et al. [20], and Young [21]. The inner part of the frame was designed to minimize unwanted (dead space) volume by following the facial landmarks and minimize frame

height. For the personalized NIV cushion, we developed a plugin for Rhinoceros (Robert McNeel & Associates, USA, available on request). In this software, the facial 3D scan can be uploaded, and eight facial landmarks are then selected manually (see Supplemental material, Additional file 1: Figure S7). Based on the input, the Rhinoceros software produces a mask curve and automatically selects a 3D cushion model according to the nasion–pogonion distance. For this exploratory study, two different mask sizes (small and large) were chosen for each test head model: the size automatically chosen by the software and one size smaller, to examine the accuracy of the sizing system. The files,

which were saved as an STL format, could be sliced and exported to a 3D printer.

The masks are stabilized and fixated to the patient's head using a 3D printed holder (PC-ISO, Fortus 450mc, Stratasys, Israel) and headgear with five fixation points (Respireo SOFT nasal masks from Air Liquide Healthcare, France), as described previously [6].

Mask production

The frames were 3D printed in VeroClear material (Objet30, Stratasys, Israel). The frame rings were 3D printed in PC-ISO material (Fortus 450mc, Stratasys, Israel). The personalized cushions were 3D printed in three different biocompatible (a minimum of ISO 10993-5 and 10993-10) soft materials:

1. Silicone urethane (SU) (Sil30, A-35, Carbon 3D, USA) on a DLS printer (M3 Max, Carbon3D, USA), resulting in two masks: SU_{small} and SU_{large} .
2. Silicone (Amsil 20501, A-50, Elkem Silicones, Norway) on a FDM printer (3D4Makers, Netherlands and Purpose AM Systems, Latvia), resulting in two masks: Si_{small} and Si_{large} .
3. Soft photopolymer resin (MED414, A-50, Loctite, Henkel, Germany) on a DLP printer (OriginOne, Stratasys, Israel), resulting in two masks: SPR_{small} and SPR_{large} .

Figure 2 shows examples of masks produced in these different soft materials.

NIV simulation

Pediatric NIV was simulated in a bench test to determine the performance of the produced personalized masks. As a comparison for the personalized masks, the only commercial oronasal NIV mask available in our PICU

(Nivairo, Fisher & Paykel Healthcare, New Zealand, size: XS, which is the smallest available) was also tested. The setup consisted of a head model connected to a mechanical lung simulator (Michigan Instruments, Grand Rapids, USA) (Fig. 1). The test lung simulator was set at 25 ml/cmH₂O compliance and 20 cmH₂O parabolic resistance. These settings were fixed during all NIV simulation test runs. The mask was placed and fixated to the head model, and connected to a ventilator (Hamilton C6 ventilator, Hamilton Medical, Switzerland) by a standard dual limb breathing circuit (Fisher&Paykel Healthcare, New Zealand). A standard computer was used to continuously collect the flow (31 Hz), volume (31 Hz), airway pressure (31 Hz) and air leak (2 Hz) data from the ventilator using the Hamilton DataLogger software and to collect the facial surface pressure (2 Hz) data using custom-made software in Python.

For ventilation, the respiratory rate was set on 20 breaths per minute, with an inspiration–expiration ratio of 1:3 in NIV-ST modus, which delivers time-cycled, pressure-supported breaths. The ventilator parameters and facial surface pressures were then measured for 90 s, which thus included analysis of a total of 30 breaths, for three consecutive ventilator pressure steps, noted as peak-inspiratory pressure/positive end-expiratory pressure: 15/5 cmH₂O, 20/5 cmH₂O, 25/10 cmH₂O. For each of these three ventilator pressure steps, we performed three independent measurements (triplicate). Between these measurements, the mask was removed from the head model, re-fixated and the headbands were re-adjusted.

Performance outcomes

To examine the performance of the masks, air leak percentage (L_{air} , reported by the ventilator as $V_{leak}\%$, which is automatically derived per breath by one minus



Fig. 2 An overview of the personalized cushion materials. From left to right: silicone urethane (SU) printed on a DLS printer, silicone (Si) printed on an FDM printer, and soft photopolymer resin (SPR) printed on a DLP printer

the calculated exhaled volume divided by inhaled volume, multiplied by 100%), facial surface pressure (N/cm²) on the nose bridge (P_{nb}), pressure on the chin (P_c) and average pressure (P_{av}, calculated as the mean from all six pressure sensors) of the masks were compared.

Statistical analysis

Data on the performance outcomes for each mask were collected three times in independent measurements for 30 breaths, and summarized into mean values per measurement. These data are presented as medians (IQR) for each mask per ventilator pressure step. No sample size calculation regarding the number of head models was performed for this exploratory preclinical bench study. Comparisons between multiple mask types were analyzed using the Friedman test for non-parametric repeated measures data due to the small sample size and absence of normal distribution upon graphical histogram presentation or the Shapiro–Wilk test. If this test yielded a significant *p*-value (<0.05), Wilcoxon signed-rank tests were executed as post hoc comparison between the masks. IBM SPSS Statistics (version 28) was used for the analysis.

Results

All three soft materials were successfully 3D printed and could be assembled into NIV oronasal masks with an airtight, biocompatible personalized soft cushion. Total production time of these masks was below 15 h: the SU masks (small and large) took around 11 h (2 h to print, 1 h of manual post-processing and 8 h of curing); Si masks (small and large) took 15 (11 h of printing, 4 h of curing and 15 min of post-processing); SPR masks (small and large) took 10 h (9 h to print and 1 h of post-processing and curing).

Air leak performance was generally acceptable for all personalized masks (Fig. 3), and there were no relevant differences between the different head models. Overall, L_{air} was below 30%, except at the 25/10 cmH₂O ventilation pressure step. In comparison, the commercial oronasal mask (Nivairo) showed leak percentages of >60% in two test head models (DS and CFCS) even when strapping the headgear to its limits, and >95% in the VCFS model. In the latter model no sufficient contact of the commercial mask with the face was possible. This caused disruption of the flow and pressure levels in such a way that no reliable NIV could be simulated. At all three ventilator pressure steps (15/5, 20/5 and 25/10 cmH₂O) all personalized masks had lower L_{air} as compared to the

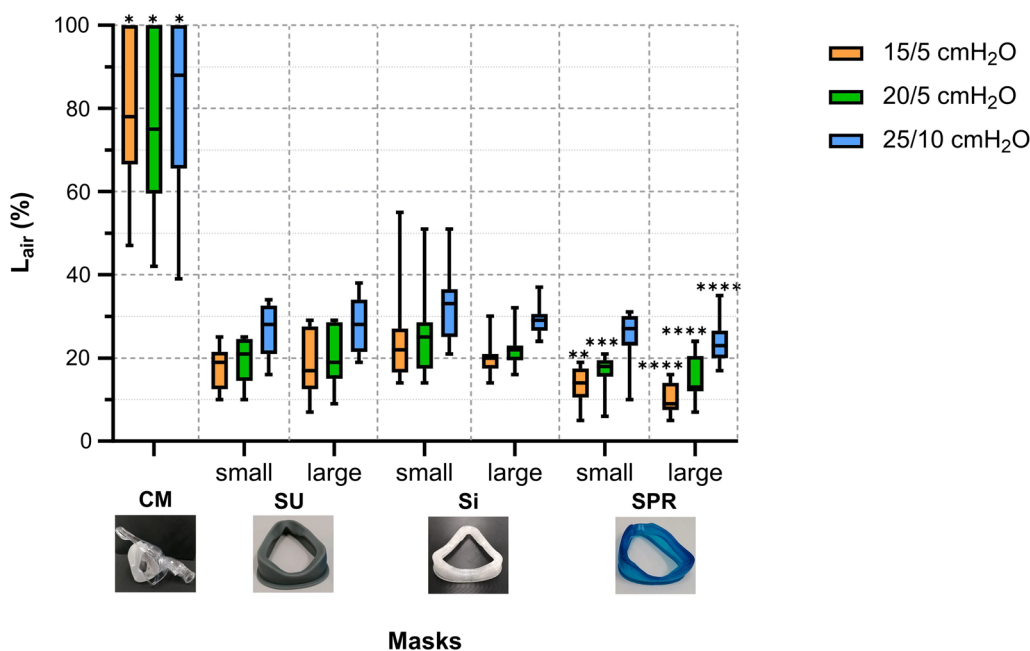


Fig. 3 Air leak percentages (L_{air}) for the commercial mask (CM) and each personalized non-invasive ventilation (NIV) mask (silicone urethane (SU) small and large; silicone (Si) small and large; and soft photopolymer resin (SPR) small and large) during pediatric NIV bench test simulation at three different ventilation pressure steps (peak-inspiratory pressure/positive end-expiratory pressure: 15/5 cmH₂O, 20/5 cmH₂O and 25/5 cmH₂O). The boxplots and error-bars depict median/IQR and range, respectively. *CM versus SU_{small}, SU_{large}, Si_{small}, Si_{large}, SPR_{small} and SPR_{large} (*p* < 0.05); **SPR_{small} versus Si_{small} and Si_{large} (*p* < 0.05); ***SPR_{small} versus Si_{small} (*p* < 0.05); ****SPR_{large} versus Si_{small} and Si_{large} (*p* < 0.05) as analyzed by Friedman non-parametric test with post hoc testing

commercial mask (Fig. 3). Moreover, there was a small benefit in the SPR masks as compared to the Si masks. The data on L_{air} per test head model are presented in Additional file 1: Figure S8 and examples of the ventilator waveforms are shown in Additional file 1: Figure S9.

Median facial surface pressure values from the personalized masks were below 0.50 N/cm^2 at $15/5 \text{ cmH}_2\text{O}$ ventilator pressure step (Fig. 4). Surface pressure delivered to the nose bridge was relatively high as compared to the chin region. Only P_{nb} showed significant differences between the masks. Herein, the commercial mask resulted in significantly lower facial pressure than SU_{small} , SU_{large} , Si_{small} , Si_{large} and SPR_{small} , while values for SPR_{large} were lower than SU_{small} and Si_{small} . However, as the commercial mask did not make sufficient contact with the face in the case of the VCFS model, data for this test head were omitted from the analysis. Additional file 1: Figure S10 shows P_{nb} , P_{chin} and P_{av} for each ventilator pressure step. The data on facial pressure per test head model are presented in Additional file 1: Figure S11.

Discussion

The aim of the current study was to test the air leak and facial surface pressure performance of personalized oronasal NIV face masks using different 3D printed soft materials. In this proof-of-concept bench simulation of

pediatric NIV using head models of young children with abnormal facial characteristics, we show that it is possible to obtain biocompatible, personalized mask cushions with acceptable air leak and surface pressure performance using a relatively short and semi-automated production process.

To our knowledge this study is the first to examine different 3D printed biocompatible soft materials to develop personalized NIV masks for children, aimed at supporting critically ill children with acute respiratory failure. For application in the acute setting, personalized masks should be rapidly and readily available after initial stabilization with commercial NIV masks or alternative interfaces. As such, ideally the total production time of a personalized mask should be as low as possible, with little hands-on time to decrease the need for available or specialized personnel. For this purpose, the relatively novel technique of 3D printing soft, biocompatible materials holds much promise [22, 23]. It is believed that this method provides a benefit as compared to recent studies that used molding techniques [9, 24], or that used 3D printing of rigid materials [18, 25]. In our current production process, we were able to develop personalized NIV masks within a 12-h time window (the SPR mask). Considering that a facial 3D scan by handheld devices can be made within 60 s, and can be uploaded into our

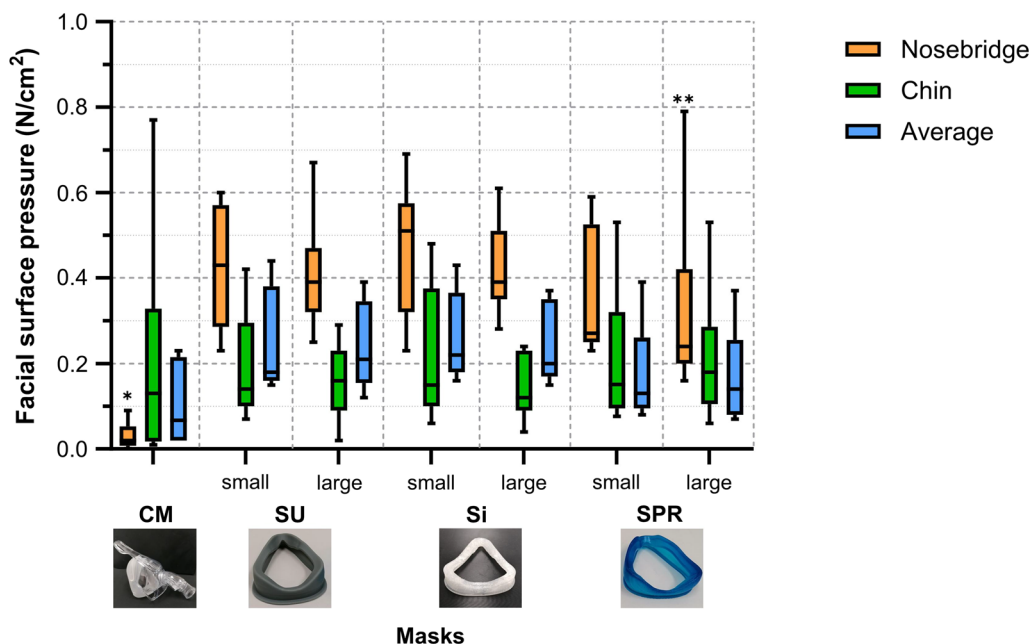


Fig. 4 Facial surface pressures (N/cm^2) (average for all six sensors, nose bridge and chin region) for the commercial mask (CM) and each personalized non-invasive ventilation (NIV) mask (silicone urethane (SU) small and large; silicone (Si) small and large; and soft photopolymer resin (SPR) small and large) during pediatric NIV bench test simulation at a peak-inspiratory pressure of $15 \text{ cmH}_2\text{O}$ and a positive end-expiratory pressure of $5 \text{ cmH}_2\text{O}$. The boxplots and error-bars depict median/IQR and range, respectively. *CM versus SU_{small} , SU_{large} , Si_{small} , Si_{large} and SPR_{small} ($p < 0.05$); ** SPR_{large} versus SU_{small} and Si_{small} ($p < 0.05$)

semi-automated software for mask selection, ongoing medical device development appears justified. However, before implementing personalized NIV masks in critically ill children, pilot (first-in-human) and subsequent clinical testing is warranted. It will, in particular, be important to identify pediatric patient subgroups (e.g., young age) that will most likely benefit the greatest of personalized masks in terms of NIV success. In this light, it is important to note that the syndromes associated with facial abnormalities included in our study were chosen to facilitate proof-of-concept, but do not necessarily represent populations receiving more specific attention.

In terms of air leak, all personalized NIV masks, performed to an acceptable degree (leak percentage generally below 30%) [26] in our bench test using head models with specific facial features. The observed air leak was significantly lower in the personalized interfaces versus the commercial mask and among the personalized mask there appeared to be a small advantage of the masks with photopolymer resin material (the SPR mask). In case of the SPR_{large} mask, the median (IQR) L_{air} was as low as 9 (8–14)%. Although moderate air leak is usually compensated for by ventilators, in particular with pressure targeted ventilation [10], large unintentional leak can result in decreased patient–ventilator synchronization, discomfort (e.g., by air flow to the eyes) and reduced alveolar ventilation, subsequently contributing to treatment failure [11, 13, 26, 27]. To reduce air leak from an ill-fitted mask, a common maneuver by nurses in daily practice is to tighten the mask headgear straps. This has the downside to increase pressure applied to the skin, contributing to development of painful sores [8]. On the other side, too low leak percentages due to a personalized fit may carry the increased risk for rebreathing of CO₂ [10, 28].

Impaired facial skin integrity during NIV in children, resulting in painful sores and ulcers, is a common complication due to high mask pressure [7]. Overall, in our model the personalized oronasal masks resulted in average surface pressures below the capillary pressure of 0.44 N/cm² (33 mmHg) in our head models, which is deemed necessary to prevent pressure injury [29]. Here, also the SPR masks slightly performed better in comparison to the other soft materials. This average pressure was comparable to that exerted by the very thin, soft silicone texture of the commercial mask. Nevertheless, in the personalized masks, the pressure at the nose bridge in some measurements exceeded this threshold. Previous studies on facial pressures of NIV masks in adults reported pressures on the nose bridge of 0.3–1.4 N/cm² [30]. Compared to these values, a median of 0.24 N/cm² (IQR 0.22–0.42) of the SPR_{large} mask appears fairly low. Since the nose bridge is most prone to pressure injury [4], future personalized mask designs, including headgear

modifications, should continue to focus on lowering P_{nb} . However, it should be taken into account that there is a fine balance between air leak and skin pressure: when accepting higher leak percentages, the pressures applied to the skin could drop. Total face masks, which cover the eyes, nose and mouth, may distribute skin pressure more evenly over a larger surface excluding the nose bridge. However, in children these masks often have large air leaks at the top side, and they have the disadvantage of risk of claustrophobia and eye irritation [31]. Nasal masks, which also avoid the nose bridge region, have the clear disadvantage of increased air leak when opening the mouth, and in critically ill children with acute respiratory failure this type of mask is usually insufficient to provide high positive bi-level pressures.

This study has several limitations. First, there are several inherent difficulties with bench testing using NIV simulation [32]. While our head models were designed to evaluate air leak percentage and potential pressure applied to skin, no breathing effort or triggering, which could affect performance of the masks, was simulated. Also, the inner head design was not fully matched to normal upper respiratory tract anatomy, and we did not incorporate different mechanical properties of the simulated respiratory system in our testing. Second, movements of patients during NIV, causing shifting of masks could for obvious reasons not be simulated. For this reason, we performed multiple independent measurements with re-adjustment of the masks in between. Third, in our head models we applied a skin-like layer from silicon that resembles the elasticity of actual skin. While skin thickness varies across the face, this setup used an evenly distributed layer of 3 mm. This could lead to higher estimated pressures in softer facial areas, such as the cheeks, but also in lower estimated pressures at the chin and nose bridge. Fourth, the test setup did not include a nasogastric tube, commonly used in these patients, which may affect mask fit causing additional air leaks [33].

Conclusion

In this proof-of-concept bench simulation of pediatric NIV using head models with abnormal facial features, we report the development of 3D printed biocompatible, personalized oronasal masks that perform with acceptable air leak and facial surface pressure. Further safety and pilot research in children, along with refinement of the logistical production process, will be necessary to inform future studies that focus on the clinical (cost-)effectiveness of using personalized NIV masks in the treatment of critically ill children.

Abbreviations

PICU	Pediatric intensive care unit
NIV	Non-invasive ventilation
DS	Down syndrome
CFCS	Cardiofaciocutaneous syndrome
VCFS	Velocardiofacial syndrome
SU	Silicone urethane
Si	Silicone
SPR	Soft photopolymer resin
L _{air}	Air leakage (%)
P _{nb}	Pressure on the nose bridge (N/cm ²)
P _{chin}	Pressure on the chin (N/cm ²)
P _{av}	Average pressure (N/cm ²)

Supplementary Information

The online version contains supplementary material available at <https://doi.org/10.1186/s40635-024-00607-w>.

Additional file 1. Supplementary figures.

Acknowledgements

We thank Frank Schoenmaker of nSize (the Netherlands) and Lyé Goto (TU Delft) for expert advice on personalization strategies and developing an open source plugin for the Rhinoceros software. We also thank Anca and Florin Dumitrescu as parent advisory board members for providing valuable input and feedback on our mask and study designs.

Author contributions

RP: conceptualization, methodology, data collection, statistical analysis, writing and editing draft. RKB: conceptualization, methodology, editing draft. MvG: conceptualization, methodology, editing draft. DM: conceptualization, methodology, editing draft. PH: providing 3D scans, editing draft. PB: methodology. TD: methodology. JdJ: methodology. PH: methodology. JvW: editing draft. CD: conceptualization, methodology, editing draft. RB: conceptualization, methodology, editing draft.

Funding

This research is funded by the Innovation Award Amsterdam UMC, the Emma Children's Hospital Foundation, the Cornelia Foundation, and Vermas Foundation.

Availability of data and materials

The datasets used and/or analyzed during the current study, as well as our developed plugin for mask design are freely available upon reasonable request.

Declarations**Ethics approval and consent to participate**

The 3D images used for the development of the test head models were obtained with approval of the Joint Research and Ethics Committee of the Eastman Dental Institute/Eastman Dental Hospital Ethics Committee (JREC 00/EO42).

Consent for publication

Not applicable.

Competing interests

The authors declare that they have no competing interests.

Author details

¹Pediatric Intensive Care Unit, Emma Children's Hospital, Amsterdam UMC, Location AMC, University of Amsterdam, Meibergdreef 9, 1105 AZ Amsterdam, The Netherlands. ²Amsterdam Reproduction and Development Research Institute, Amsterdam, The Netherlands. ³Nuffield Department of Women's and Reproductive Health, University of Oxford, Oxford, UK. ⁴Big Data Institute, Old Road Campus, University of Oxford, Oxford, UK. ⁵Department for Medical

Innovation and Development, Amsterdam University Medical Centers, Amsterdam, The Netherlands.

Received: 17 November 2023 Accepted: 22 February 2024

Published online: 01 March 2024

References

- Kneyber MCJ, de Luca D, Calderini E, Jarreau PH, Javouhey E, Lopez-Herce J, Hammer J, Macrae D, Markhorst DG, Medina A, Pons-Odena M, Racca F, Wolf G, Biban P, Brierley J, Rimensberger PC, section Respiratory Failure of the European Society for Paediatric Neonatal Intensive Care (2017) Recommendations for mechanical ventilation of critically ill children from the Paediatric Mechanical Ventilation Consensus Conference (PEM-VECC). *Intensive Care Med* 43(12):1764–1780. <https://doi.org/10.1007/s00134-017-4920-z>
- Barker N, Willox M, Elphick H (2018) A review of the benefits, challenges and the future for interfaces for long term non-invasive ventilation in children. *Int J Respir Pulm Med*. <https://doi.org/10.23937/2378-3516/1410077>
- Emeriaud G, Pons-Odena M, Bhalla AK, Shein SL, Killien EY, Modesto IAV, Rowan C, Baudin F, Lin JC, Gregoire G, Napolitano N, Mayordomo-Colunga J, Diaz F, Cruces P, Medina A, Smith L, Khemani RG, Pediatric Acute Respiratory Distress Syndrome Epidemiology Investigators Pediatric Acute Lung Injury Sepsis Investigators Network (2023) Noninvasive ventilation for pediatric acute respiratory distress syndrome: experience from the 2016/2017 pediatric acute respiratory distress syndrome incidence and epidemiology prospective cohort study. *Pediatr Crit Care Med* 24(9):715–726. <https://doi.org/10.1097/PCC.0000000000003281>
- Brill AK, Pickersgill R, Moghal M, Morrell MJ, Simonds AK (2018) Mask pressure effects on the nasal bridge during short-term noninvasive ventilation. *ERJ Open Res*. <https://doi.org/10.1183/23120541.00168-2017>
- Wu YY, Acharya D, Xu C, Cheng B, Rana S, Shimada K (2018) Custom-fit three-dimensional-printed BiPAP mask to improve compliance in patients requiring long-term noninvasive ventilatory support. *J Med Device* 12(3):0310031–0310038. <https://doi.org/10.1115/1.4040187>
- Hovenier R, Goto L, Huysmans T, van Gestel M, Klein-Blommert R, Markhorst D, Dijkman C, Bem RA (2022) Reduced air leakage during non-invasive ventilation using a simple anesthetic mask with 3D-printed adaptor in an anthropometric based pediatric head-lung model. *Front Pediatr*. <https://doi.org/10.3389/fped.2022.873426>
- Fedor KL (2017) Noninvasive respiratory support in infants and children. *Respir Care* 62(6):699–717. <https://doi.org/10.4187/respcare.05244>
- Visscher MO, White CC, Jones JM, Cahill T, Jones DC, Pan BS (2015) Face masks for noninvasive ventilation: fit, excess skin hydration, and pressure ulcers. *Respir Care* 60(11):1536–1547. <https://doi.org/10.4187/respcare.04036>
- Bockstedte M, Xepapadeas AB, Spintzyk S, Poets CF, Koos B, Aretxabaleta M (2022) Development of personalized non-invasive ventilation interfaces for neonatal and pediatric application using additive manufacturing. *J Pers Med*. <https://doi.org/10.3390/jpm12040604>
- Elliott MW (2004) The interface: crucial for successful noninvasive ventilation. *Eur Respir J* 23(1):7–8. <https://doi.org/10.1183/09031936.03.00115.903>
- Hess DR (2011) Patient–ventilator interaction during noninvasive ventilation. *Respir Care* 56(2):153–165. <https://doi.org/10.4187/respcare.01049>
- Bedi PK, DeHaan K, Ofosu D, Olmstead D, MacLean JE, Castro-Codesal M (2023) Predictors of NIV-related adverse events in children using long-term noninvasive ventilation. *Pediatr Pulmonol*. <https://doi.org/10.1002/ppul.26689>
- Oto J, Chenelle CT, Marchese AD, Kacmarek RM (2014) A comparison of leak compensation during pediatric noninvasive ventilation: a lung model study. *Respir Care* 59(2):241–251. <https://doi.org/10.4187/respcare.02616>
- Morris JV, Ramnarayan P, Parslow RC, Fleming SJ (2017) Outcomes for children receiving noninvasive ventilation as the first-line mode of mechanical ventilation at intensive care admission: a propensity score-matched cohort study. *Crit Care Med* 45(6):1045–1053. <https://doi.org/10.1097/CCM.0000000000002369>

15. Goutman SA, Chen L, Plott JS, Vankoevinger KK, Kurili A, Shih AJ, Green GE (2021) A personalized approach to non-invasive ventilation masks in amyotrophic lateral sclerosis using facial scanning and 3D-printing. *Ann 3D Printed Med*. <https://doi.org/10.1016/j.stlm.2021.100027>
16. Shikama M, Nakagami G, Noguchi H, Mori T, Sanada H (2018) Development of personalized fitting device with 3-dimensional solution for prevention of NIV oronasal mask-related pressure ulcers. *Respir Care* 63(8):1024–1032. <https://doi.org/10.4187/respcare.05691>
17. Borrás-Novell C, Causapie MG, Murcia M, Djian D, Garcia-Algar O (2022) Development of a 3D individualized mask for neonatal non-invasive ventilation. *Int J Bioprint* 8(2):516. <https://doi.org/10.18063/ijb.v8i2.516>
18. Willox M, Metherall P, Jeays-Ward K, McCarthy AD, Barker N, Reed H, Elphick HE (2020) Custom-made 3D printed masks for children using non-invasive ventilation: a feasibility study of production method and testing of outcomes in adult volunteers. *J Med Eng Technol* 44(5):213–223. <https://doi.org/10.1080/03091902.2020.1769759>
19. DINED anthropometric database (2023) TU Delft, Delft <https://dined.iotudelft.nl/en/ellipse/tool> Accessed 25 Sep 2023
20. Goto L, Lee W, Molenbroek JFM, Cabo AJ, Goossens RHM (2019) Traditional and 3D scan extracted measurements of the heads and faces of Dutch children. *Int J Ind Ergon*. <https://doi.org/10.1016/j.ergon.2019.102828>
21. Young JW (1966) Selected facial measurements of children for oxygen-mask design. *AM Rep Apr*
22. Bachtiar EO, Erol O, Millrod M, Tao R, Gracias DH, Romer LH, Kang SH (2020) 3D printing and characterization of a soft and biostable elastomer with high flexibility and strength for biomedical applications. *J Mech Behav Biomed Mater*. <https://doi.org/10.1016/j.jmbbm.2020.103649>
23. Guttridge C, Shannon A, O'Sullivan A, O'Sullivan KJ, O'Sullivan LW (2022) Biocompatible 3D printing resins for medical applications: a review of marketed intended use, biocompatibility certification, and post-processing guidance. *Ann 3D Printed Med*. <https://doi.org/10.1016/j.stlm.2021.100044>
24. Martelly E, Rana S, Shimada K (2021) Design and fabrication of custom-fit BiPAP and CPAP masks using three-dimensional imaging and three-dimensional printing techniques. *J Med Devices*. <https://doi.org/10.1115/1.4049981>
25. Ma Z, Hyde P, Drinnan M, Munguia J (2021) Custom three-dimensional-printed CPAP mask development, preliminary comfort and fit evaluation. *J Med Devices*. <https://doi.org/10.1115/1.4050201>
26. Vignaux L, Tassaux D, Jolliet P (2007) Performance of noninvasive ventilation modes on ICU ventilators during pressure support: a bench model study. *Intensive Care Med* 33(8):1444–1451. <https://doi.org/10.1007/s00134-007-0713-0>
27. Brill AK (2014) How to avoid interface problems in acute noninvasive ventilation. *Breathe* 10(3):230–242. <https://doi.org/10.1183/20734735.003414>
28. Ferraz B, Gomes B, Esquinas AM (2023) Noninvasive ventilation-leaks compensation and clinical implications. In: Esquinas AM (ed) *Noninvasive mechanical ventilation: theory, equipment, and clinical applications*. Springer International Publishing, Cham. https://doi.org/10.1007/978-3-031-28963-7_4
29. Agrawal K, Chauhan N (2012) Pressure ulcers: back to the basics. *Indian J Plast Surg* 45(2):244–254. <https://doi.org/10.4103/0970-0358.101287>
30. Savoldi F, Svanetti L, Tsoi JKH, Gu M, Paganelli C, Genna F, Lopomo NF (2022) Experimental determination of the contact pressures produced by a nasal continuous positive airway pressure mask: a case study. *J Mech Behav Biomed Mater*. <https://doi.org/10.1016/j.jmbbm.2022.105272>
31. Mortamet G, Amaddeo A, Essouri S, Renolleau S, Emeriaud G, Fauroux B (2017) Interfaces for noninvasive ventilation in the acute setting in children. *Paediatr Respir Rev* 23:84–88. <https://doi.org/10.1016/j.prrv.2016.09.004>
32. Olivieri C, Costa R, Conti G, Navalesi P (2012) Bench studies evaluating devices for non-invasive ventilation: critical analysis and future perspectives. *Intensive Care Med* 38(1):160–167. <https://doi.org/10.1007/s00134-011-2416-9>
33. Singer P, Rattanachaiwong S (2018) To eat or to breathe? The answer is both! Nutritional management during noninvasive ventilation. *Crit Care* 22(1):27. <https://doi.org/10.1186/s13054-018-1947-7>

Publisher's Note

Springer Nature remains neutral with regard to jurisdictional claims in published maps and institutional affiliations.